

Third VOCALS Science Meeting
March 21-23, 2011, University of Miami

Large scale and mesoscale dynamics in the VOCALS region

C. Grados, A. Chaigneau, N. Dominguez,
G. Eldin, L. Vásquez, M. Le Texier



Outline

Basic Issues:

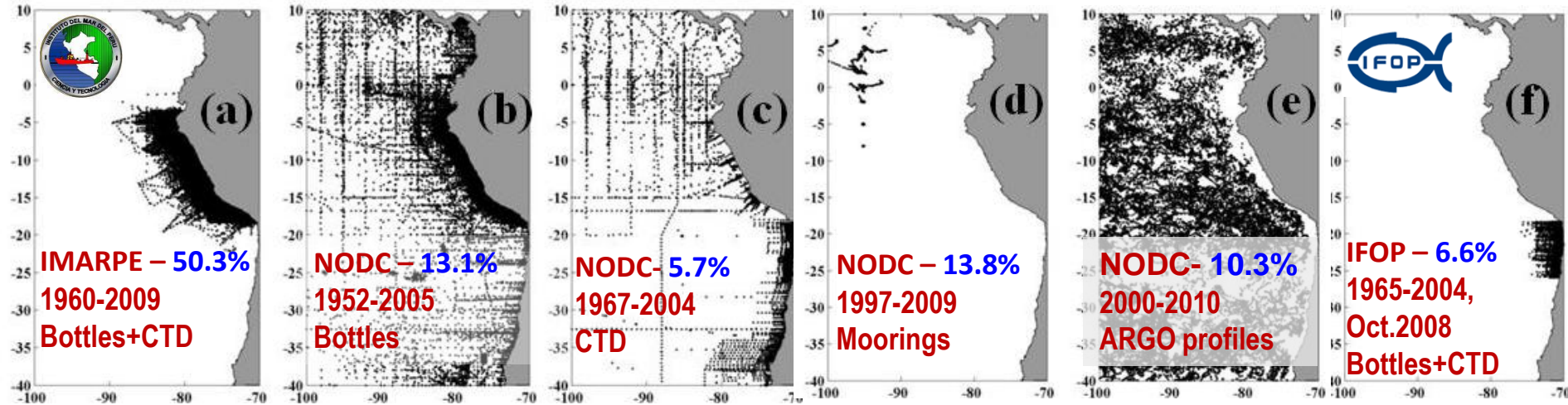
1. Contemporaneous view of the temperature and salinity fields in the North Humboldt Current System (Grados et al, in prep)
2. Vertical structure of mesoscale eddies in the VOCALS region (Chaigneau et al, submitted, JGR)

Conclusions



1. Contemporaneous view of the temperature and salinity fields

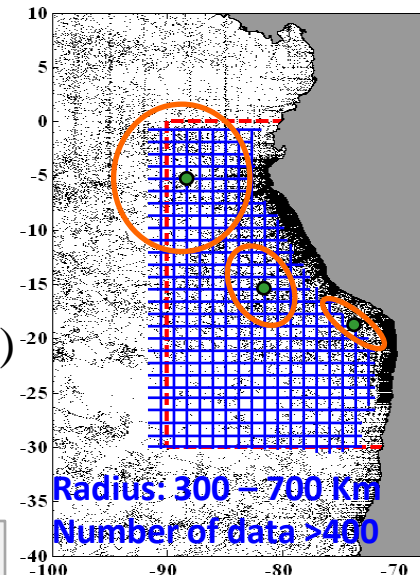
Data: 1952-2009 (IMARPE, IFOP, NODC), 142,780 T/S profiles (0-30S; 70-90W)



Methodology: CSIRO Atlas of Regional Seas (CARS, 2009); Dunn and Ridgway (2001); Ridgway et. al. (2002)

- 55 vertical levels on a $0.1^\circ \times 0.1^\circ$ horizontal grid.
- Adaptive ellipse and relatively complex weighting of the data in the ellipse.
- Adaptive-lengthscale Loess interpolation scheme with spatial (quadratic) and temporal (annual, semi-annual) components to interpolate the data at the grid points to maximise resolution in data-rich regions.

Appropriate decoupling between coastal dynamics and offshore ocean

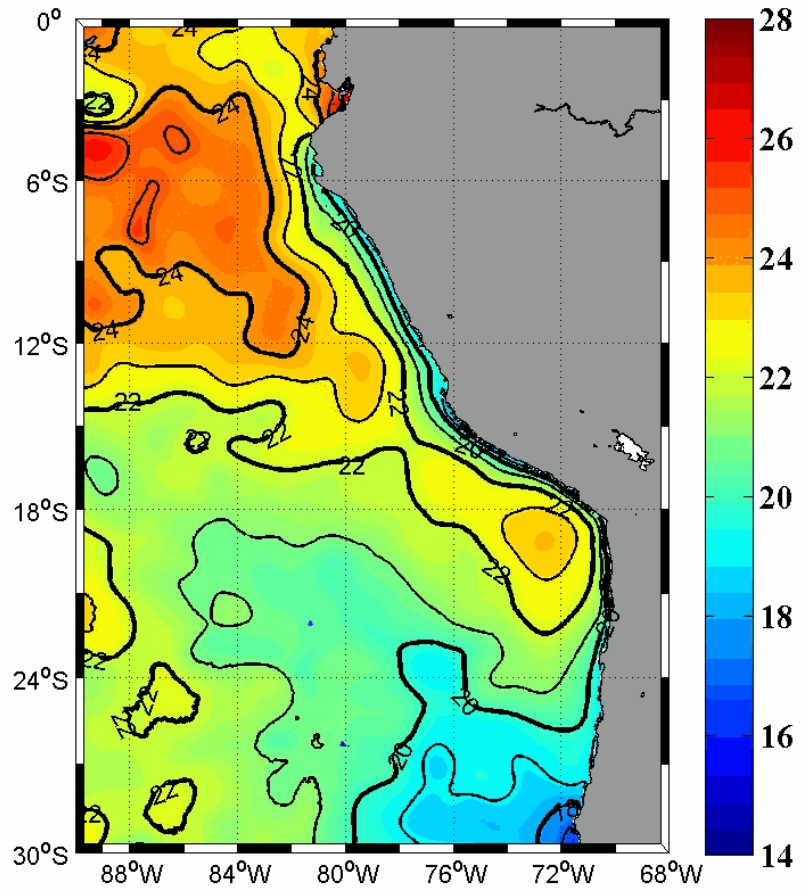


Sea surface Temperature (°C) and Salinity in the NHCS

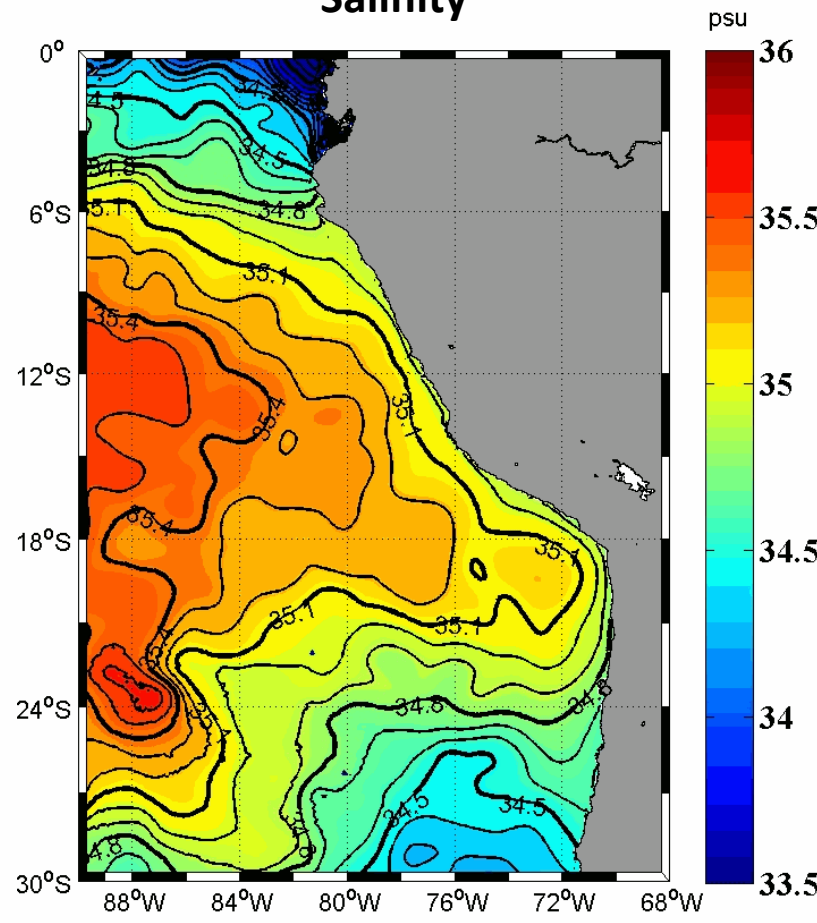
AGI - UNREGISTERED

Enero

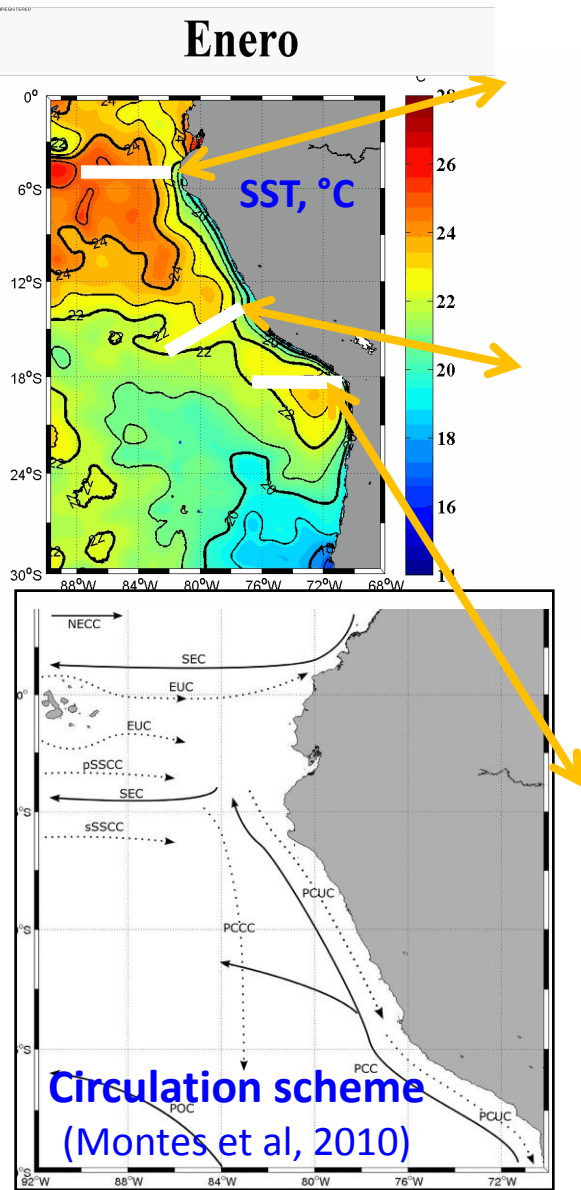
Temperature



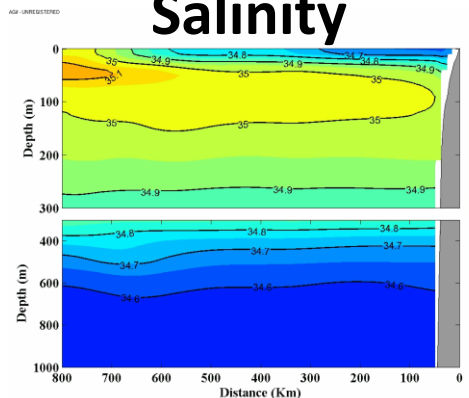
Salinity



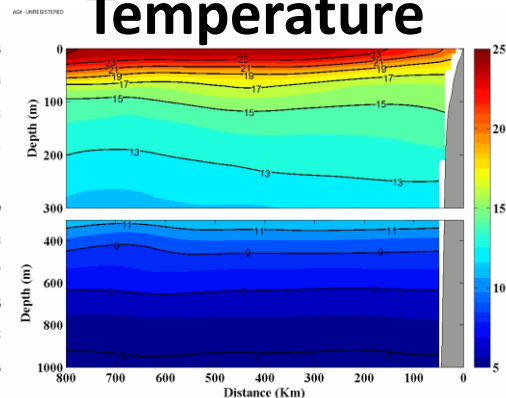
Monthly mean T/S cross-shore structure and oceanic Circulation Scheme



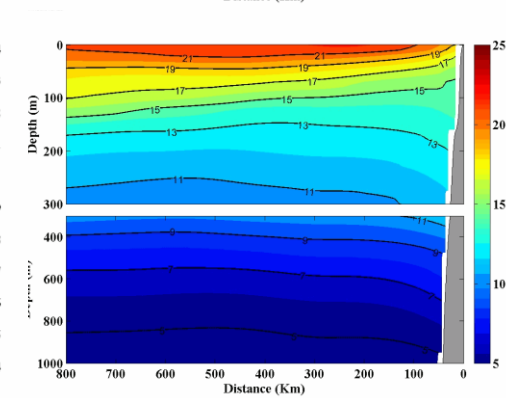
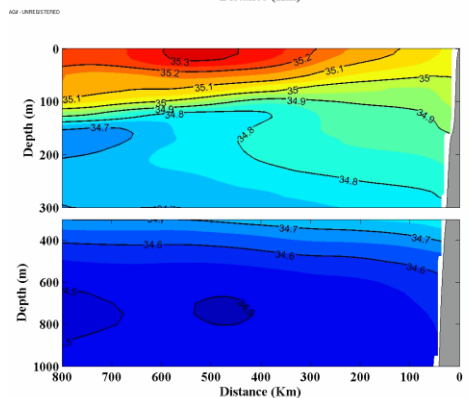
Salinity



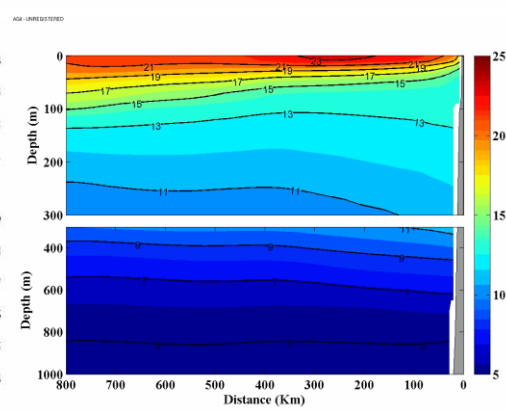
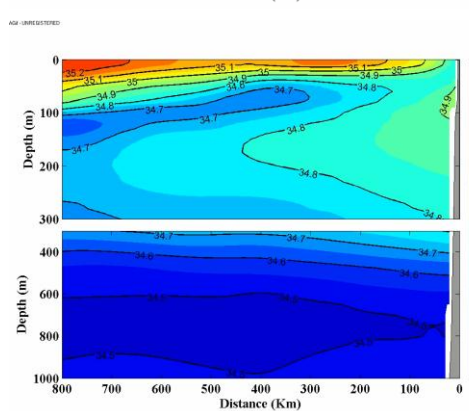
Temperaturé



**Paita
5°S**

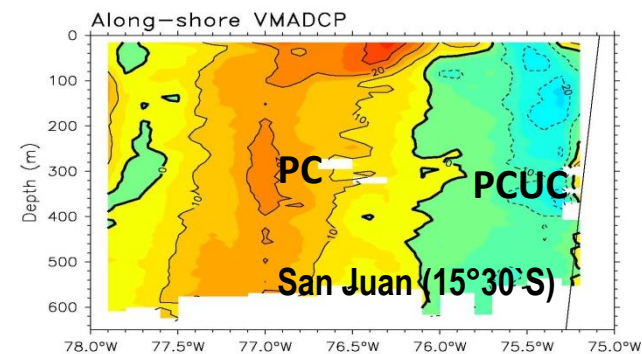
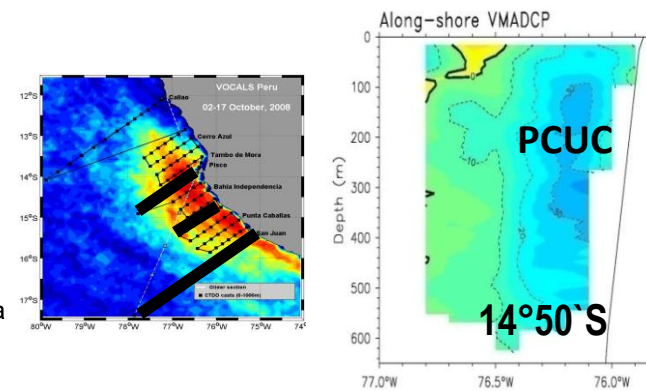
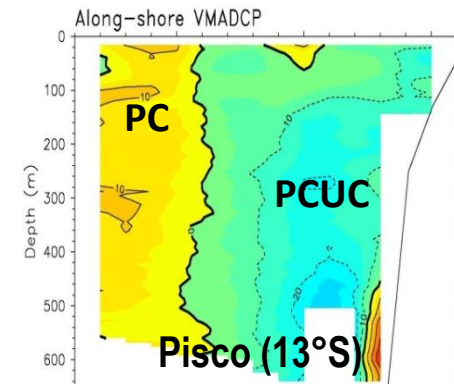
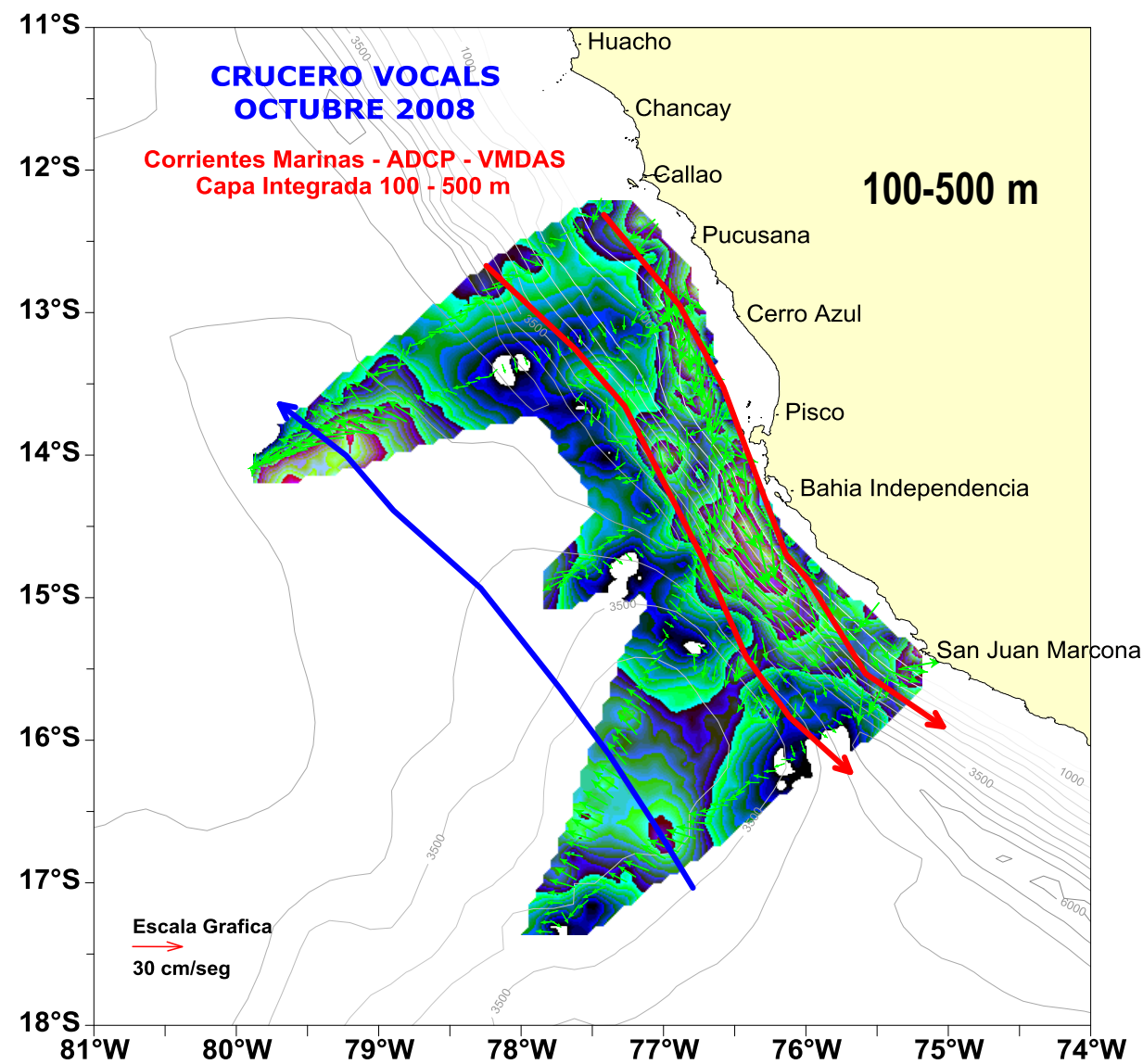


**Pisco
14°S**



**Iquique
20°S**

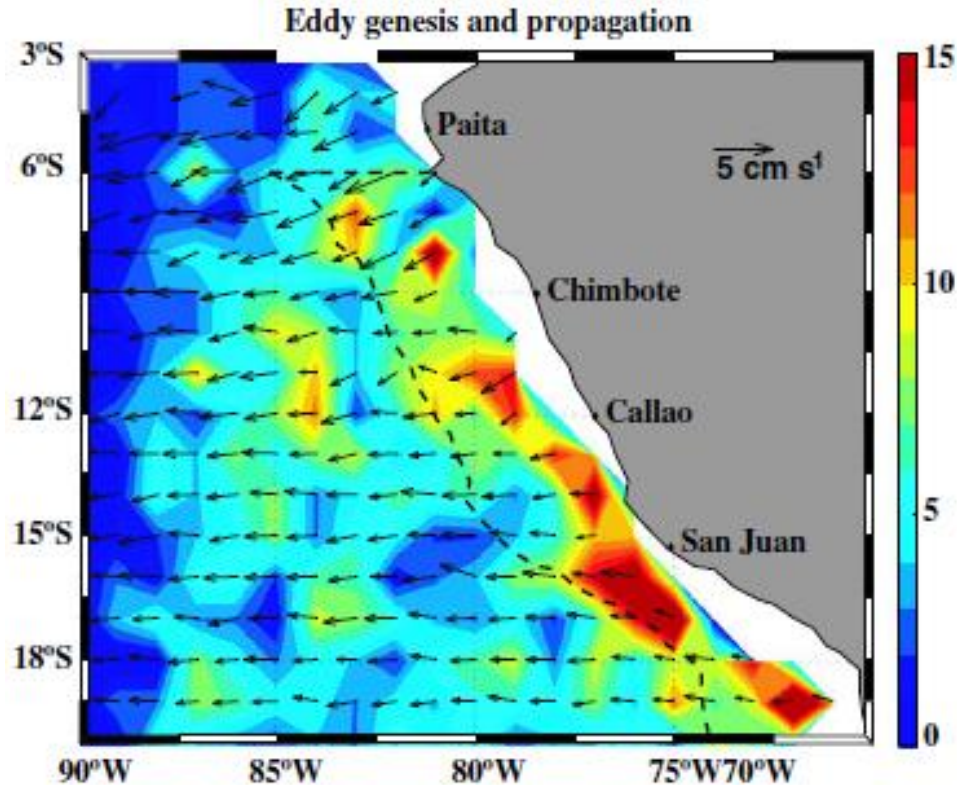
Subsurface currents from ADCP data



2. Vertical structure of mesoscale eddies

(*Chaigneau et al; submitted*)

Long-lived eddy genesis and propagation
(Chaigneau et al, 2008)

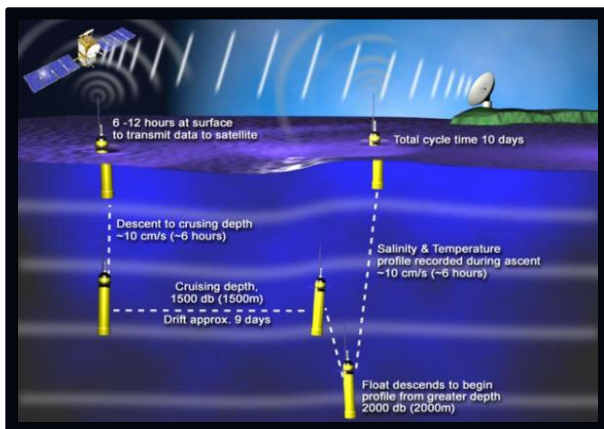


But, it is not known :

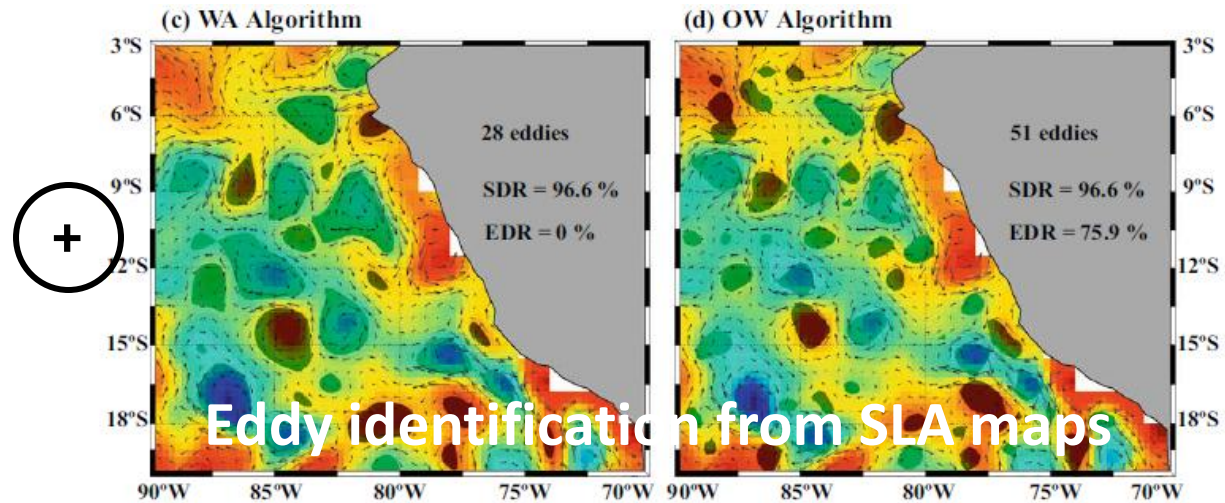
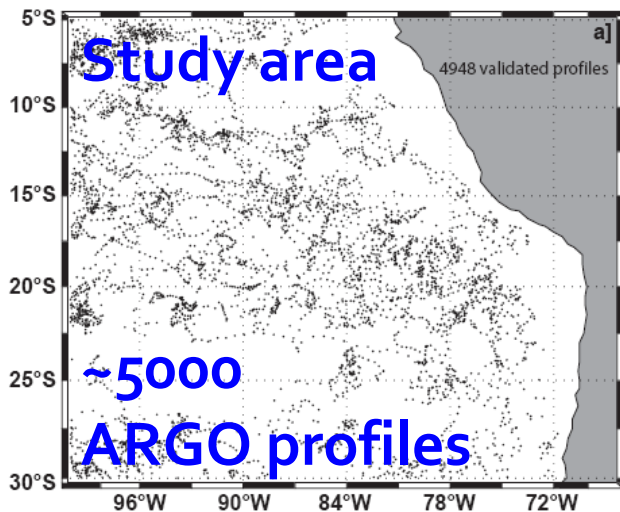
- What is the typical vertical structure of mesoscale eddies ?
- What are the associated heat and salt fluxes?
- Do cyclonic and anticyclonic eddies significantly differ?

Solution: Combine ARGO profiles and SLA maps

Methodology

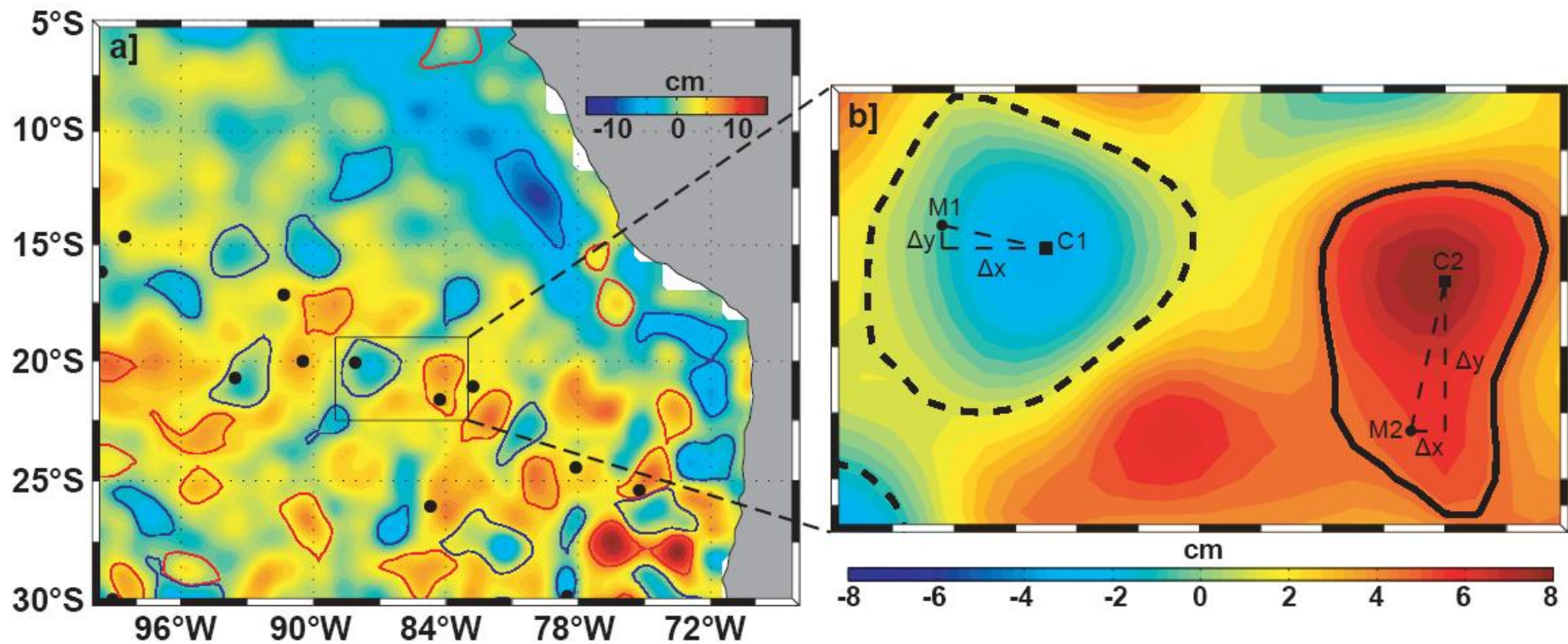


- Multi-satellites AVISO SLA maps (Oct 2000-2009).
- Eddy identification according to *Chaigneau et al. [2008; 2009]*
- Classification of the ARGO profiles depending if they surface in CE, AE, or OE.



Solution: Combine ARGO profiles and SLA maps

Example of eddy identification



Chaigneau et al., submitted

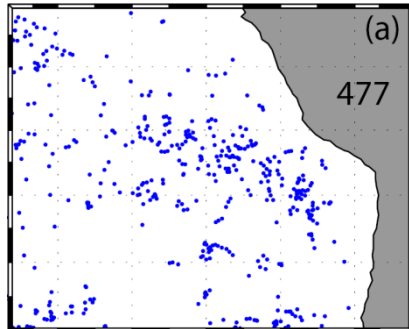
Classification and Reconstruction of composite eddies

Classification

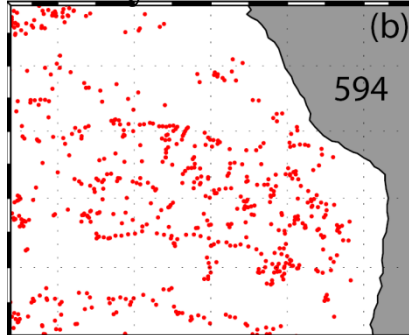


Optimum interpolation....Example at 350 m depth:

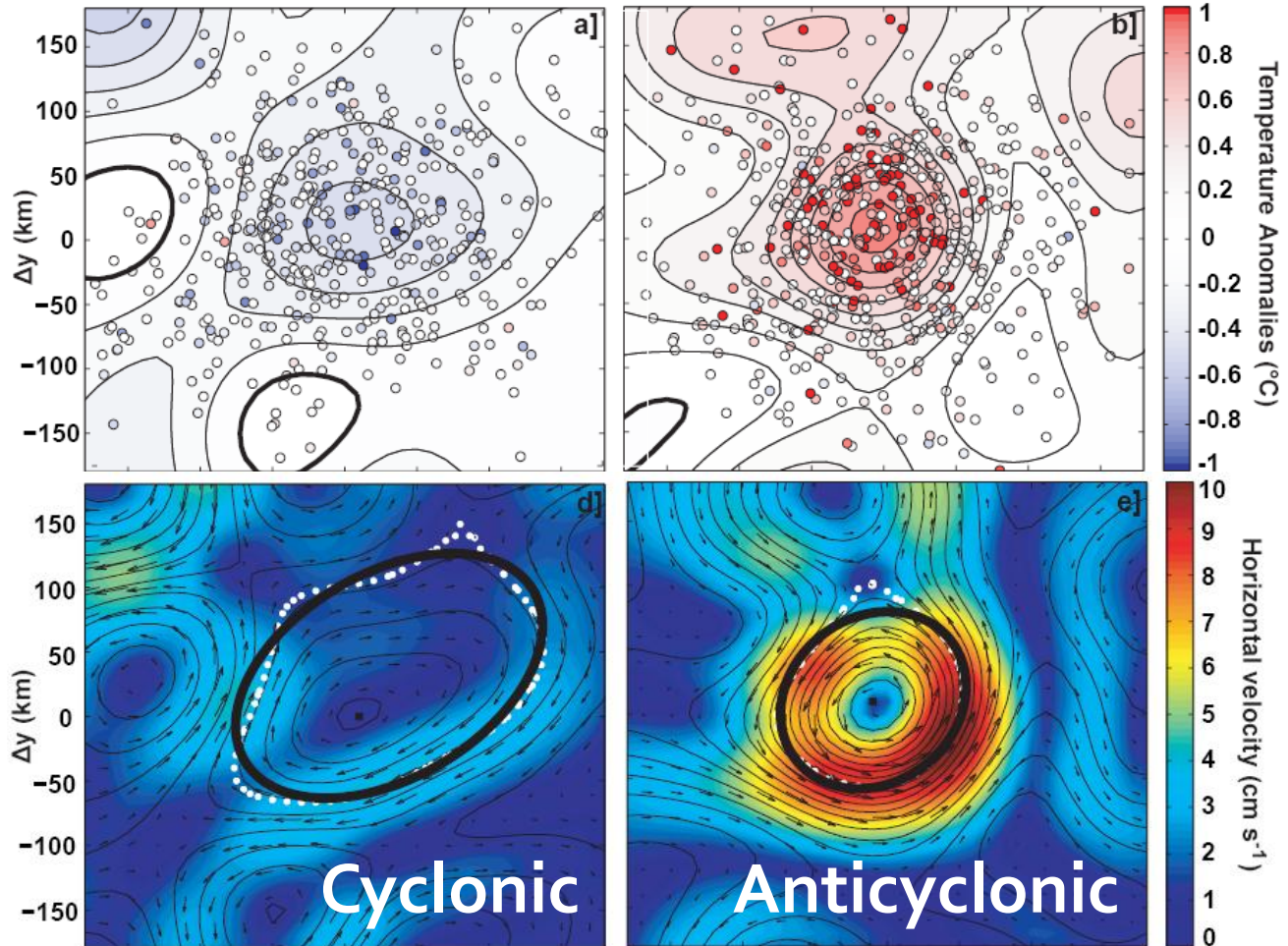
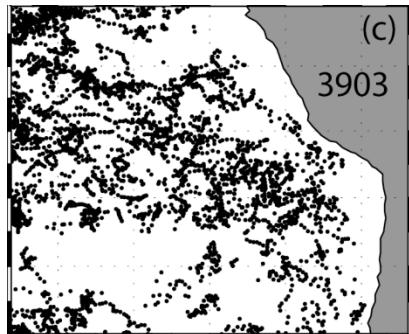
Cyclonic Eddies



Anticyclonic Eddies



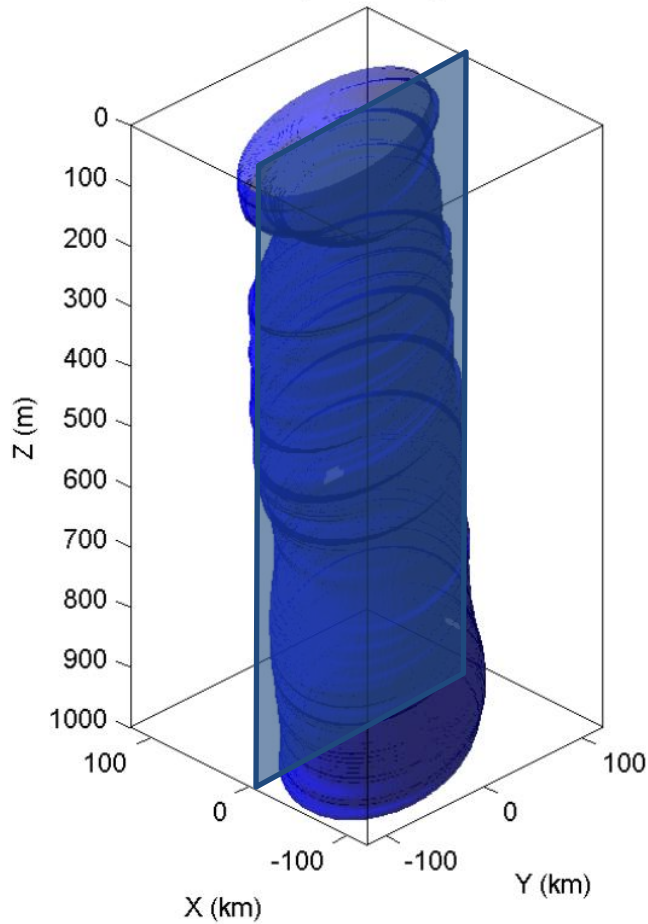
Outside Eddies



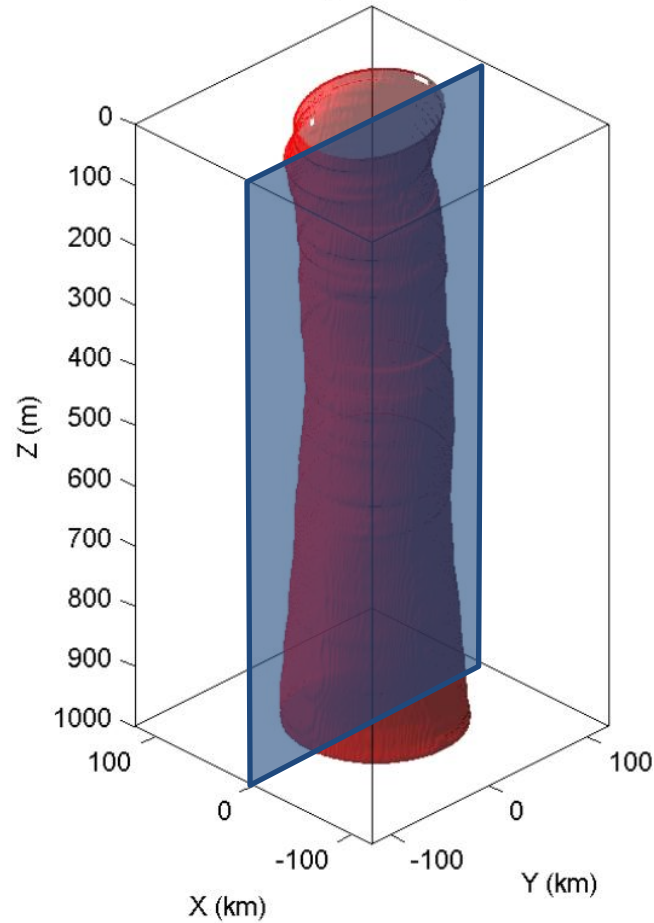
Chaigneau et al., submitted

2) Reconstruction of composite eddies

CYCLONIC

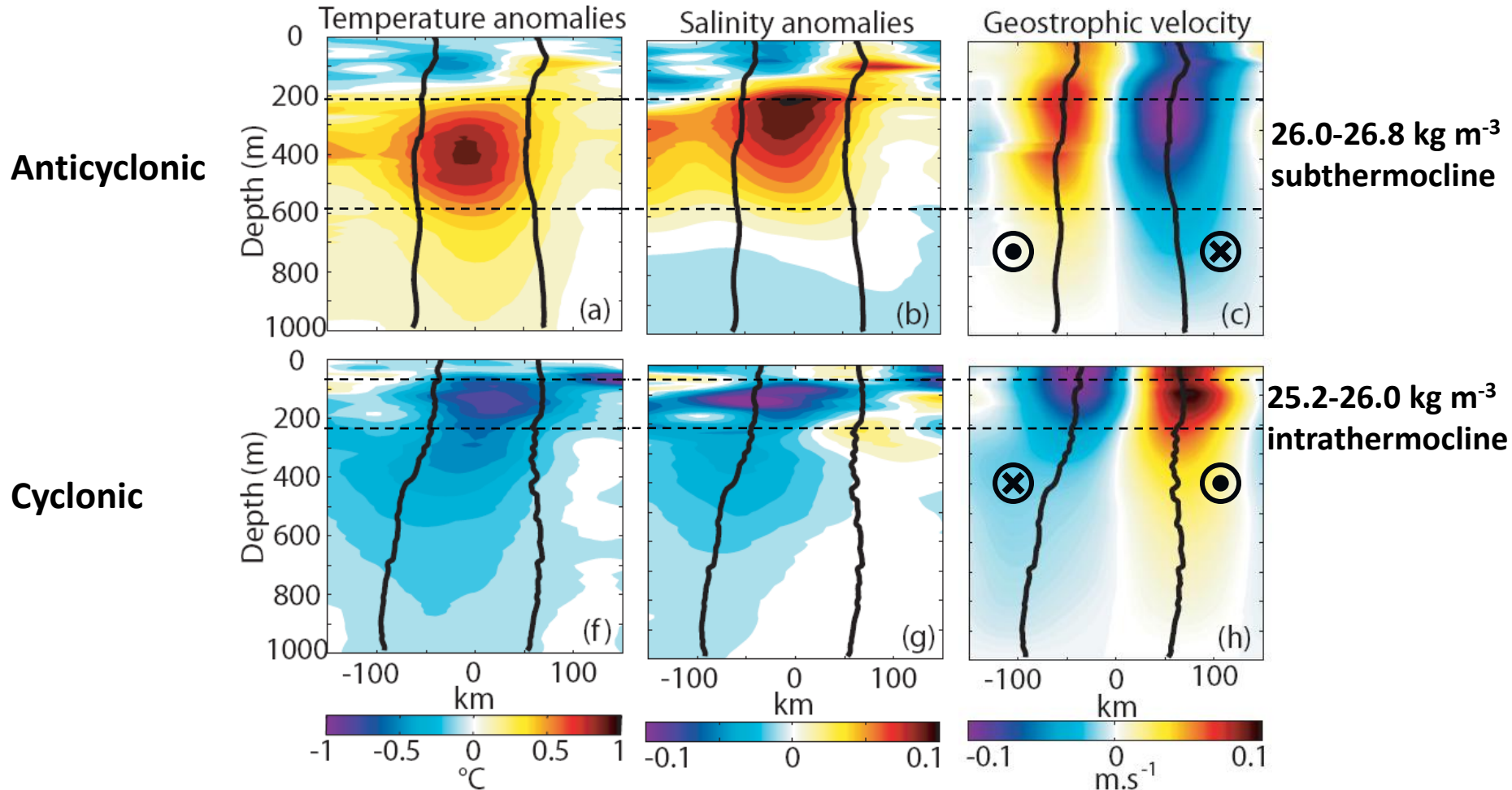


ANTICYCLONIC



Volume $\sim 10^4 \text{ km}^3$

3) Vertical section



Chaigneau et al., submitted

4) Available Heat and Salt anomalies

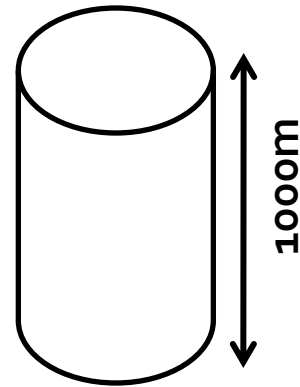
Temperature and salinity anomalies integrated over the eddy volume

$$AHA = \rho_0 c_p \int \theta' dA$$

$$ASA = 0.001 \rho_0 \int S' dA$$

	Cyclonic	Anticyclonic
AHA:	$-2.4 \times 10^{19} \text{ J}$	$2.1 \times 10^{19} \text{ J}$
ASA:	$-3.9 \times 10^{11} \text{ kg}$	$3.7 \times 10^{11} \text{ kg}$

Heat transport	$-7.6 \times 10^{11} \text{ W}$	$6.7 \times 10^{11} \text{ W}$
Salt transport	$-12.4 \times 10^3 \text{ kg s}^{-1}$	$11.7 \times 10^3 \text{ kg s}^{-1}$



→ Strong implication for the cross-shore heat and salt transport

SUMMARY

The composite analysis of the Argo profiles revealed key differences in the thermohaline vertical structure between cyclonic (CE) and anticyclonic (AE) eddies:

- The CE core is centered at ~ 100 m depth in the thermocline, the composite AE core is centered below the thermocline at ~ 400 m depth
- In the eddy core, maximum temperature and salinity anomalies are of $\pm 1^\circ\text{C}$ and ± 0.1 respectively, depending on the eddy rotation sense (positive values for AEs). Associated geostrophic swirl velocities show maximum values of order of 10 cm s^{-1} .
- Strong impact of mesoscale eddies for the cross-shore transport of heat and salt in the eastern South Pacific. In the upper 1000 m, each CE and AE have a typical volume flux of $\sim 0.7 \text{ Sv.}$, and participate to a heat and salt transport of $\pm 7 \times 10^{11} \text{ W}$ and $\pm 12 \times 10^3 \text{ kg s}^{-1}$ respectively.

ARISING QUESTIONS

What is the impact of CE and AE on the nutrients and dissolved oxygen contents, considering that on subsurface, AE cores are located within the most extended and intense OMZ?

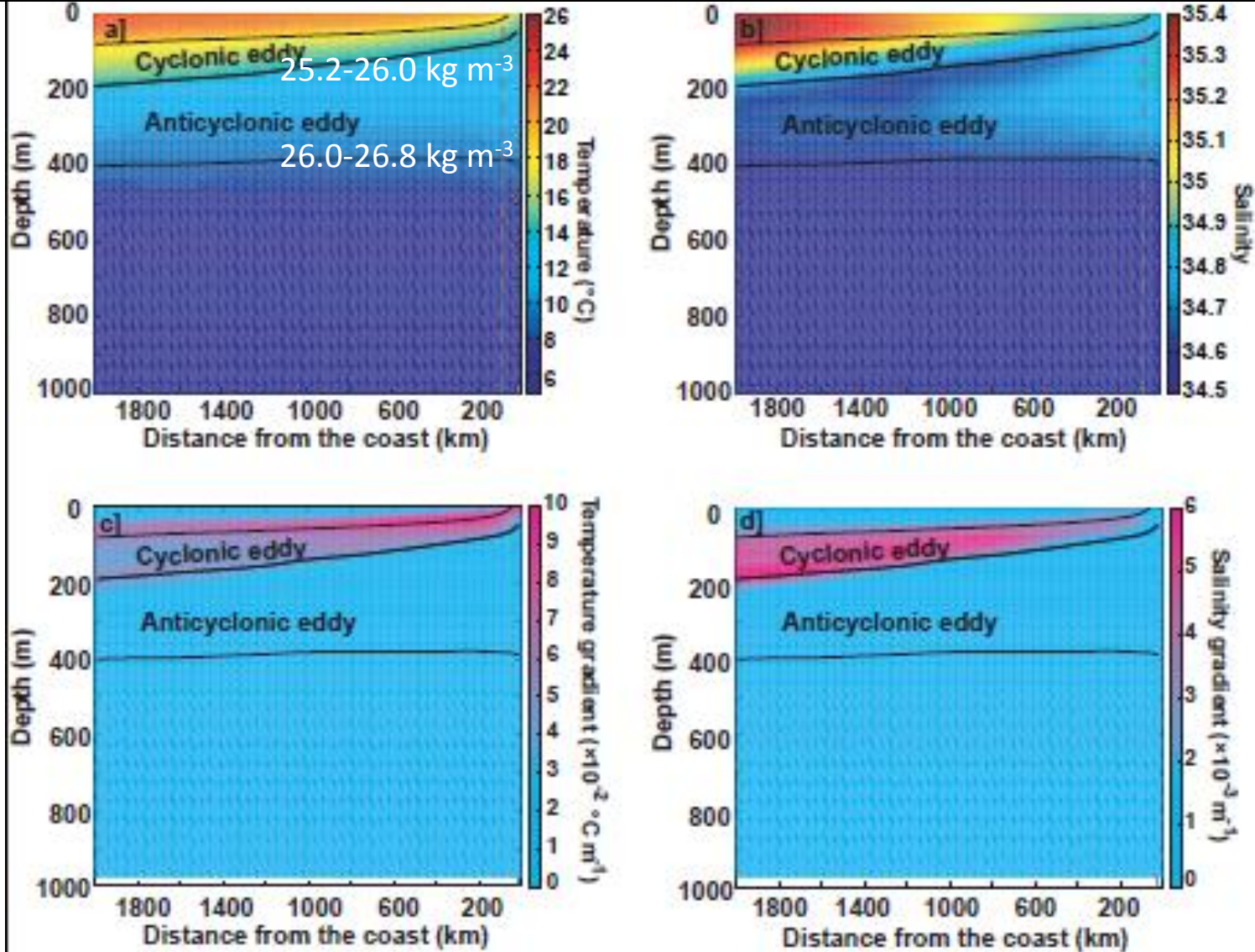
They also probably play a distinct role for the cross-shore export of DMS or terregenous particles...

Third VOCALS Science Meeting

March 21-23, 2011, University of Miami

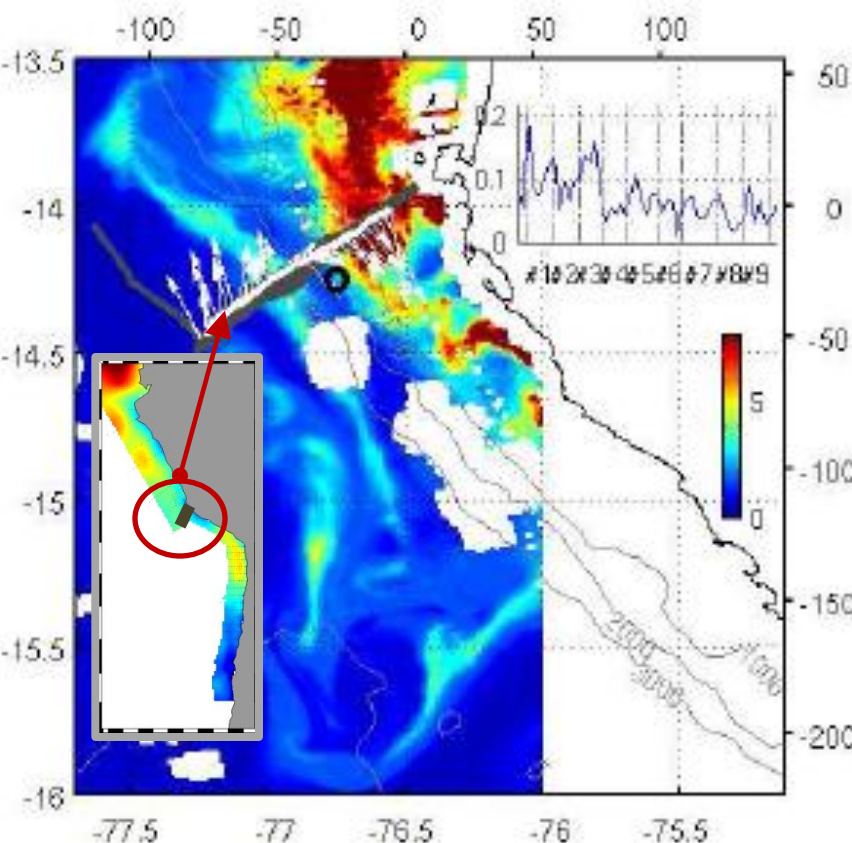


(a-b) Mean T / S sections between the coast and 2000 km offshore. The σ_θ levels (black curves) delimit vertically the composite eddy cores.

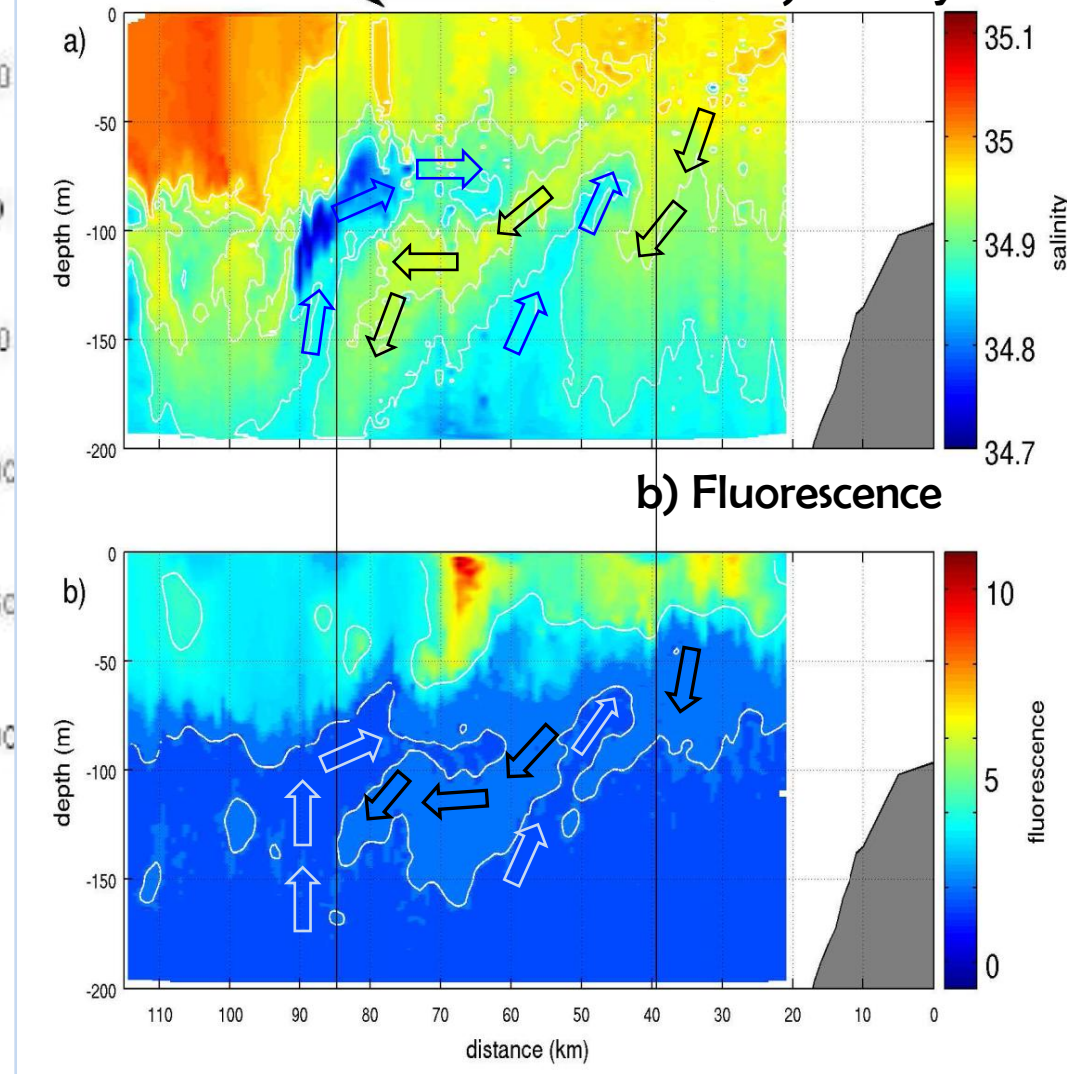


(c-d) Same as (a-b) but for the mean vertical temperature and salinity gradients which highlight the position of the eddy cores respectively to the thermocline /halocline.

The fine scale structure of the upwelling system off Pisco: Results from the VOCALS glider experiment (Pietri et al, submitted)

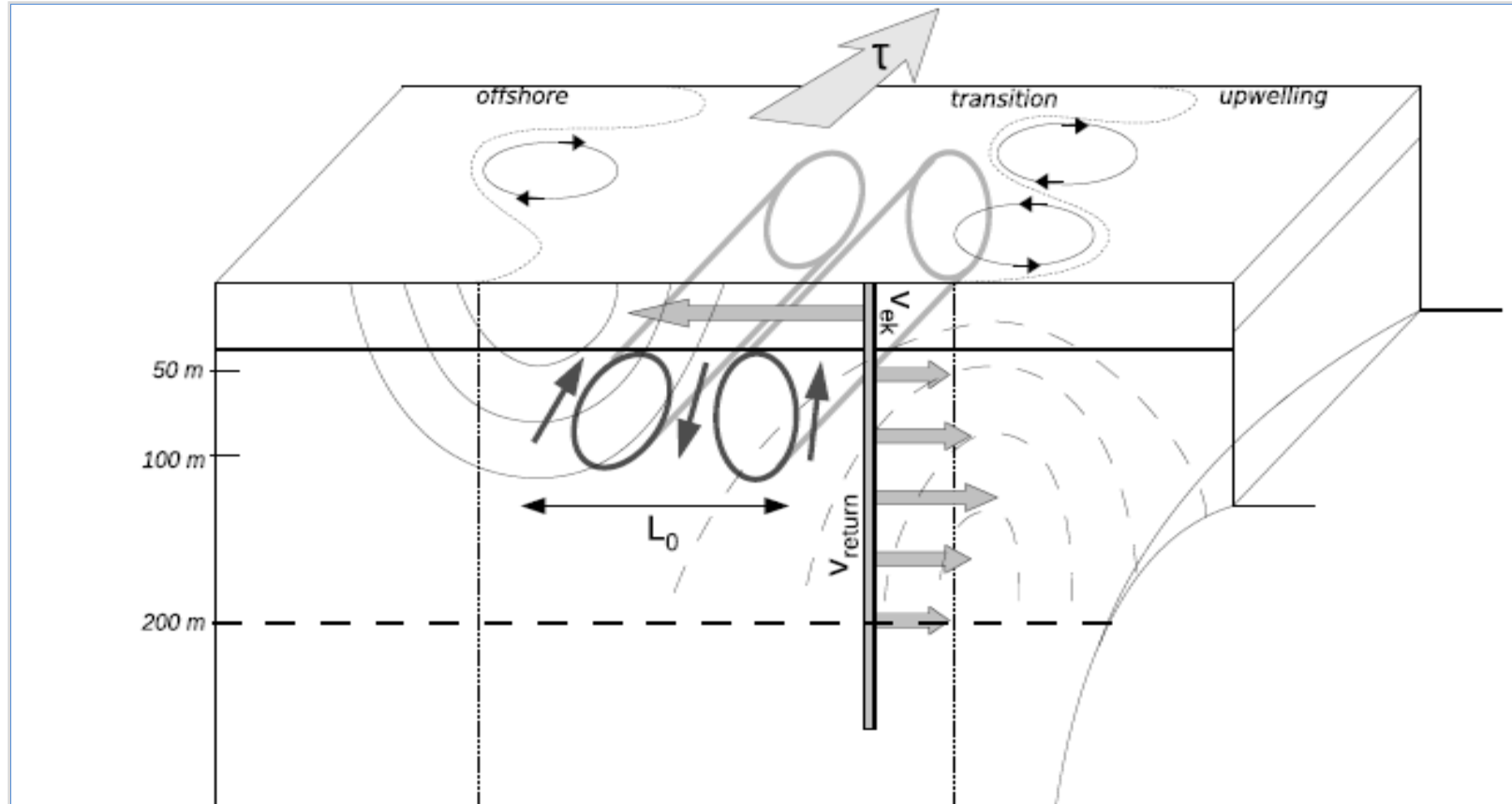


a) Ocean color satellite image (Nov. 14th-16th 2008) from "GlobColor project", glider trajectories (white line), water velocities (white arrows), data point of the Quikscat windstress (black circle); in the inset, b) Quikscat windstress time series during the glider mission.



a) salinity, b) fluorescence. Sketch of the ageostrophic secondary circulation (black arrows) and black lines marking the surface density fronts.

Cross-shore sketch of the fine scale vertical structure of the upwelling system off Pisco (14°S), as observed from glider data (Pietri et. al., submitted)



The open ocean, transition and upwelling regions are observed. The mesoscale eddies (dotted black lines), down front wind along the coast (gray arrow) driving ASC in the transition zone (gray circles), below the Ekman layer, surface current (continuing black line) and undercurrent (dashed black line) and cross-shore circulation (full array arrows).

CONCLUSIONS

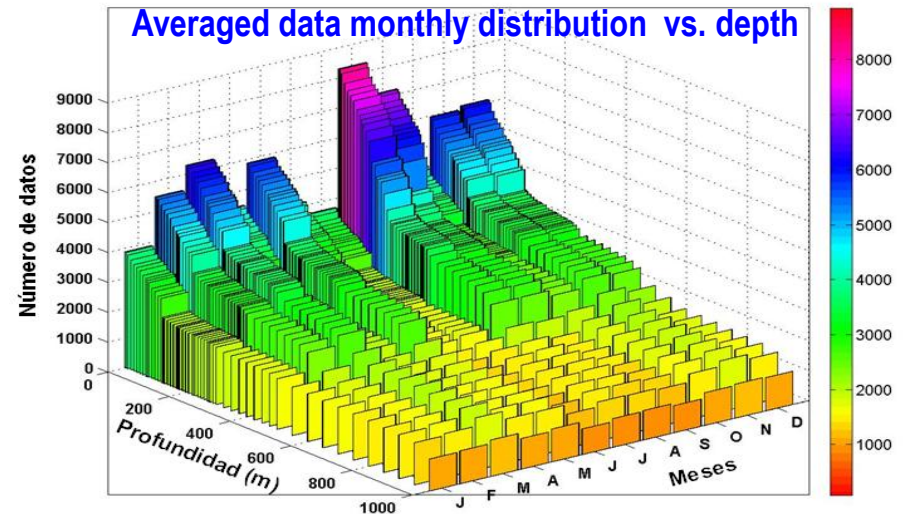
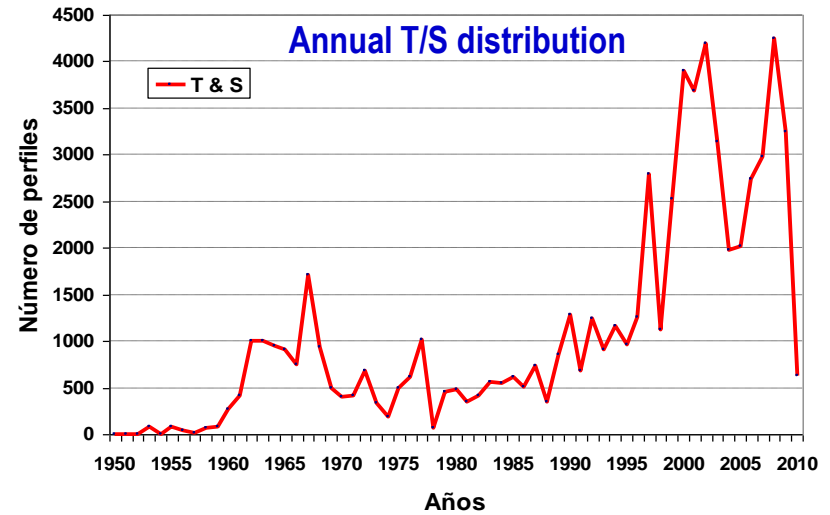
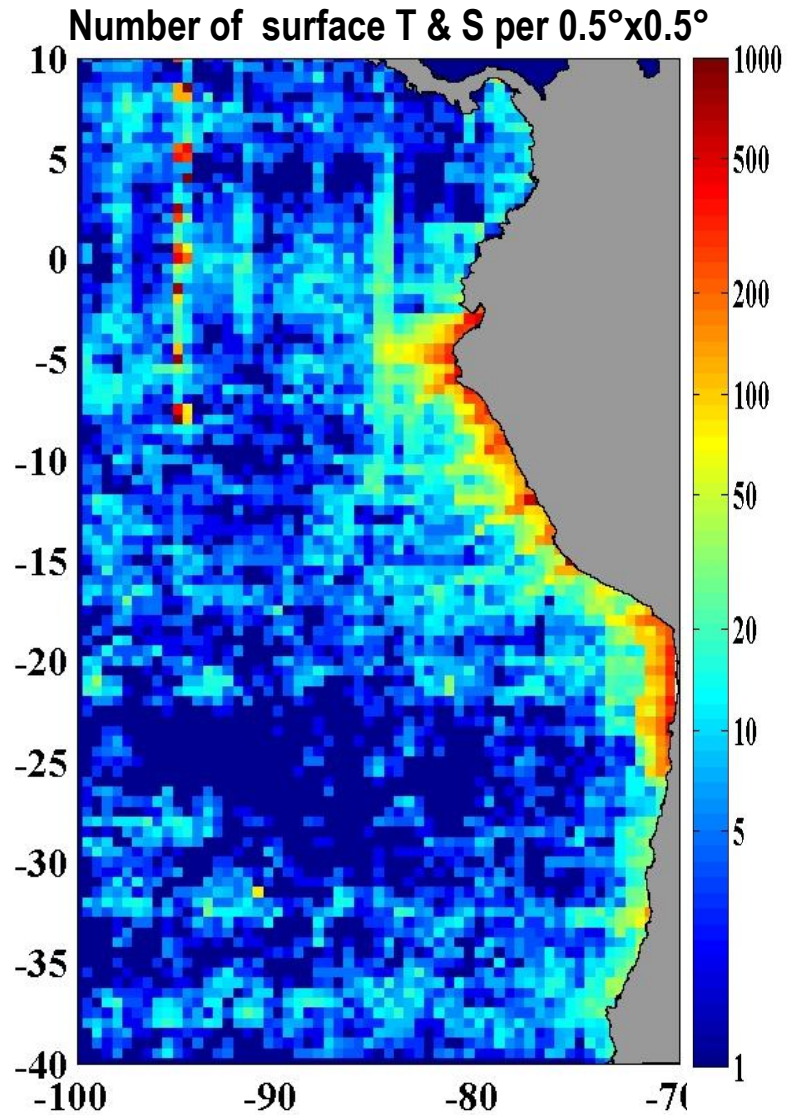
- The submesoscale structures revealed by the glider mission, were characterized by the presence of tongues of high/low salinity providing evidence of downward/upward motions, respectively, and a shoreward propagation. Considering PV, salinity and fluorescence fields, it was possible to highlight cross-shore ageostrophic circulations and corroborate the theory of Thomas and Lee (2005) on submesoscale fronts forced by down-front winds. This observational evidence suggests this instability process to be of importance in the Peru-Chile upwelling system.
- The glider experiment demonstrated that the glider technology allows to sample the boundary circulation at much better resolution than the 'Argo scale', and provide crucial information on the spatial and temporal variability in coastal upwelling regions.

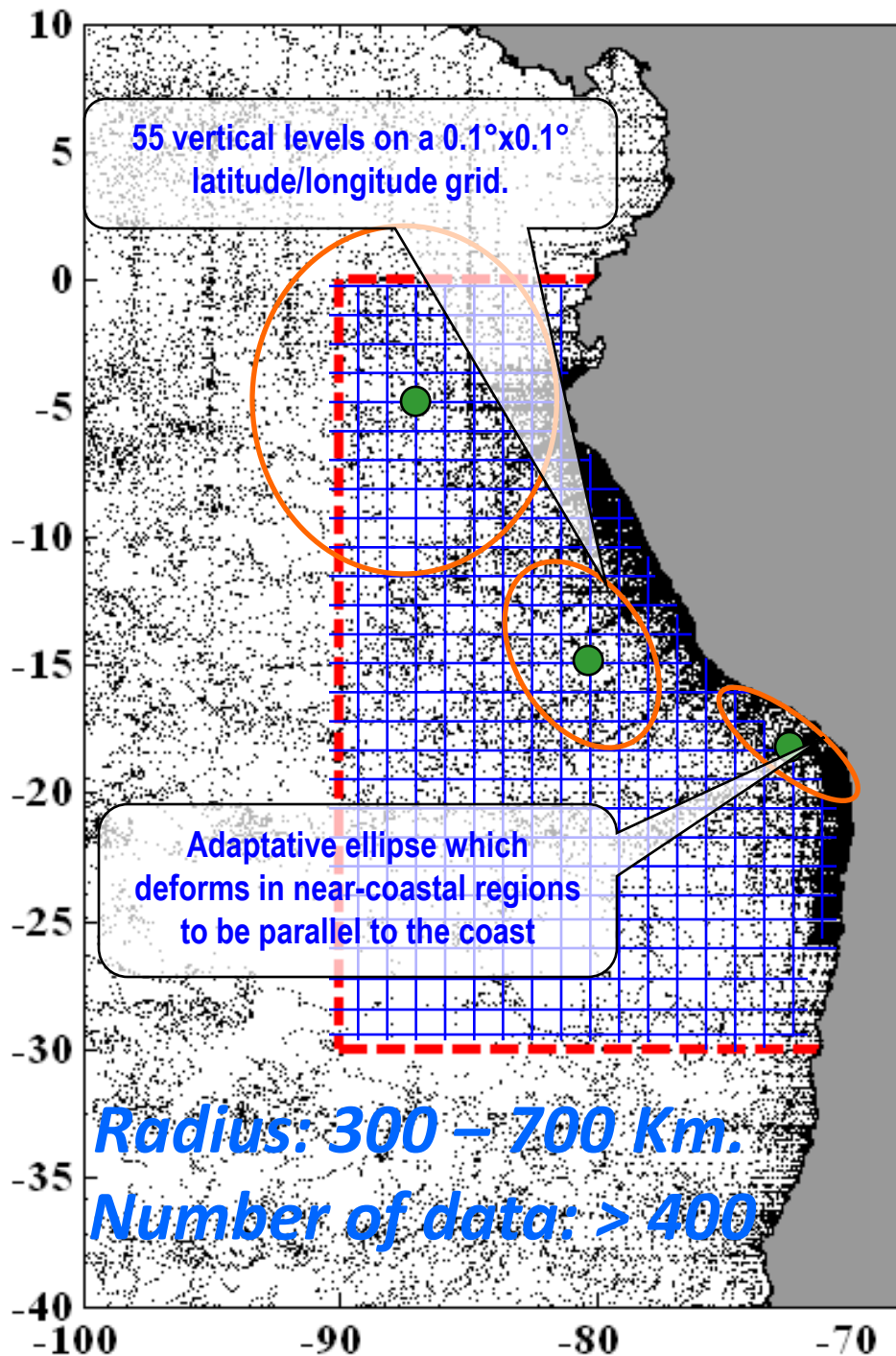
It is known that:

(Hormazabal et al., 2004; Chaigneau & Pizarro, 2005; Correa-Ramirez et al, 2007; Chaigneau et al., 2008; 2009)

- The mean eddy surface characteristics (radius, vorticity, propagation velocity, lifetime, etc.)
- Their importance for the cross-shore transport of seawater properties from coastal regions to the offshore ocean
- Their propagation patterns (generation near the coast and propagation westward) and the temporal evolution of their mean properties

Data distribution





- 55 vertical levels on a $0.1^\circ \times 0.1^\circ$ horizontal grid.

- Adaptive ellipse

- Relatively complex weighting of the data in the ellipse

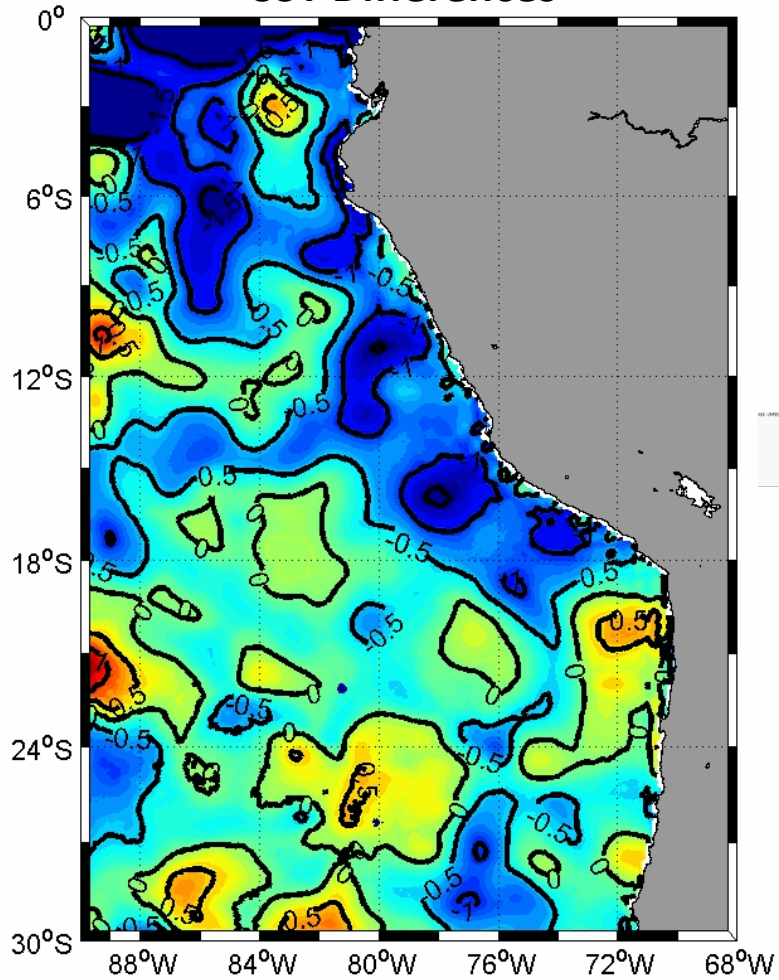
- Loess interpolation scheme with spatial (quadratic) and temporal (annual and semi-annual) components to interpolate the data at the grid points.

Better decoupling between coastal dynamics and the offshore ocean

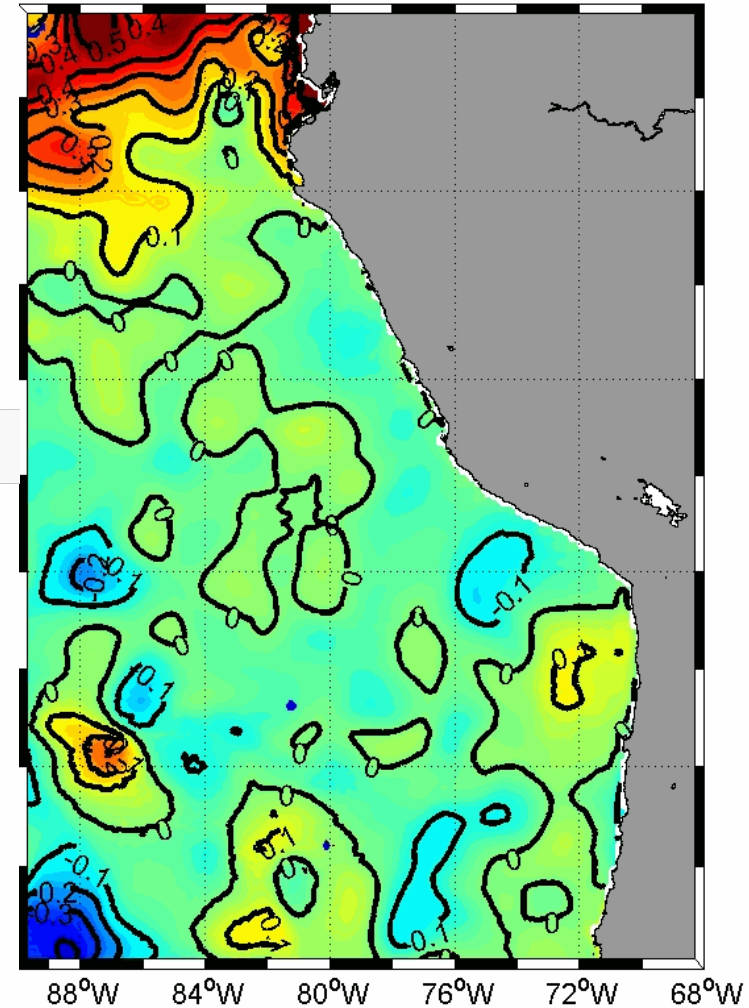
Comparison with CARS

AGIF - UNREGISTERED

SST Differences

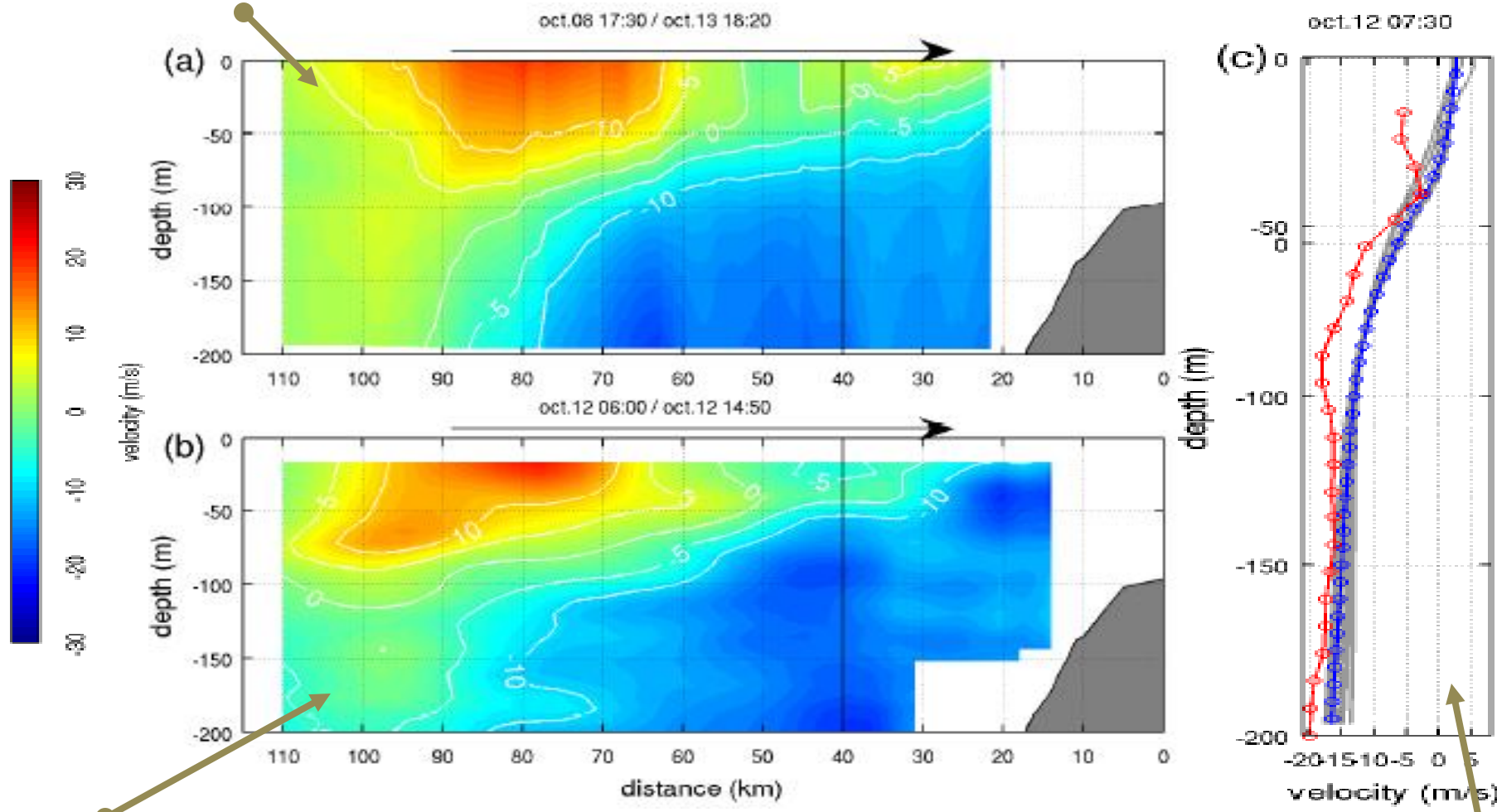


SSS Differences

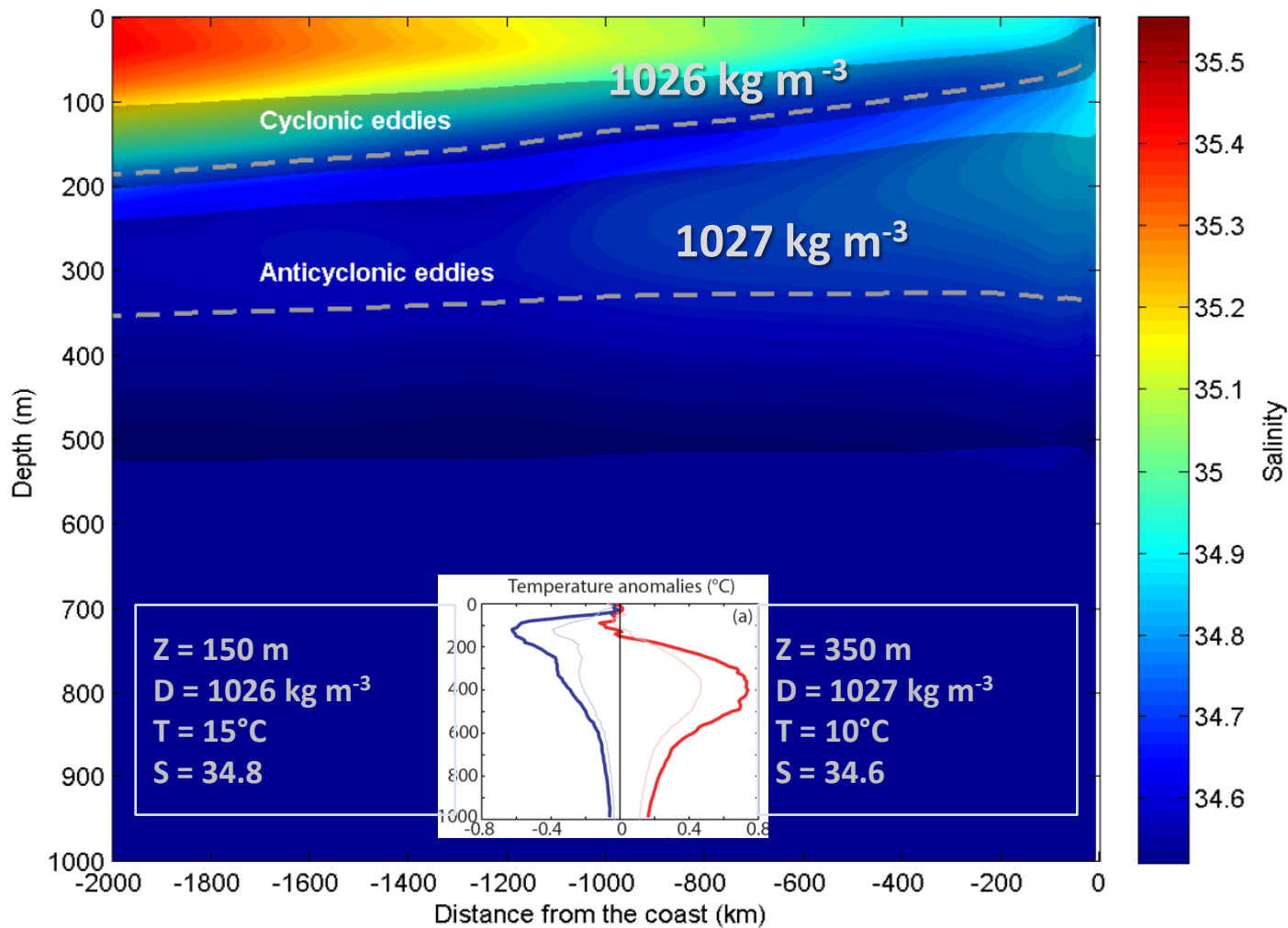


Enero

a) Absolute geostrophic velocities perpendicular to the glider section estimated from glider section #2. (Pietri et. al., submitted)



- b) ADCP currents on section #2, crossing of the glider and the ship (black line).**
- c) ADCP section corresponding to the crossing point (red) and transects (velocity) estimated from the glider data and at crossing point (blue line). Data around the crossing point (within 10 km/15 hrs) in gray lines.**



2.2. Identification algorithms and eddy property determination

Two main stages for eddy identification:

1st.- the *selection* of streamlines associated with eddies.

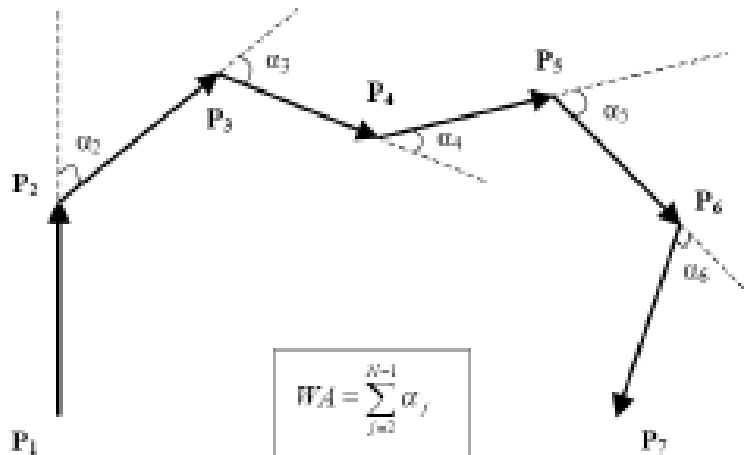
2nd.- the *clustering* of distinct streamlines corresponding to the same vortex.

The winding-angle (WA) detection algorithm

(geometrical criteria)

“A vortex exists when instantaneous streamlines mapped onto a plane normal to the vortex core exhibit a roughly circular or spiral pattern [...]”

Robinson (1991)



$$WA = \sum_{j=2}^{N-1} \langle P_{j-1}, P_j, P_{j+1} \rangle = \sum_{j=2}^{N-1} \alpha_j$$

$$\langle P_{j-1}, P_j, P_{j+1} \rangle = \alpha_j \quad \text{the signed angle between} \\ [P_{j-1} P_j] \text{ and } [P_j P_{j+1}]$$

The WA algorithm attempts to locate a vortex by selecting and clustering closed streamlines. The WA of the streamline corresponds to the cumulated sum of the angles between all pairs of consecutive segments.

2.3 Comparing eddy identification methods

The Okubo-Weiss (OW) parameter

(physical criteria)

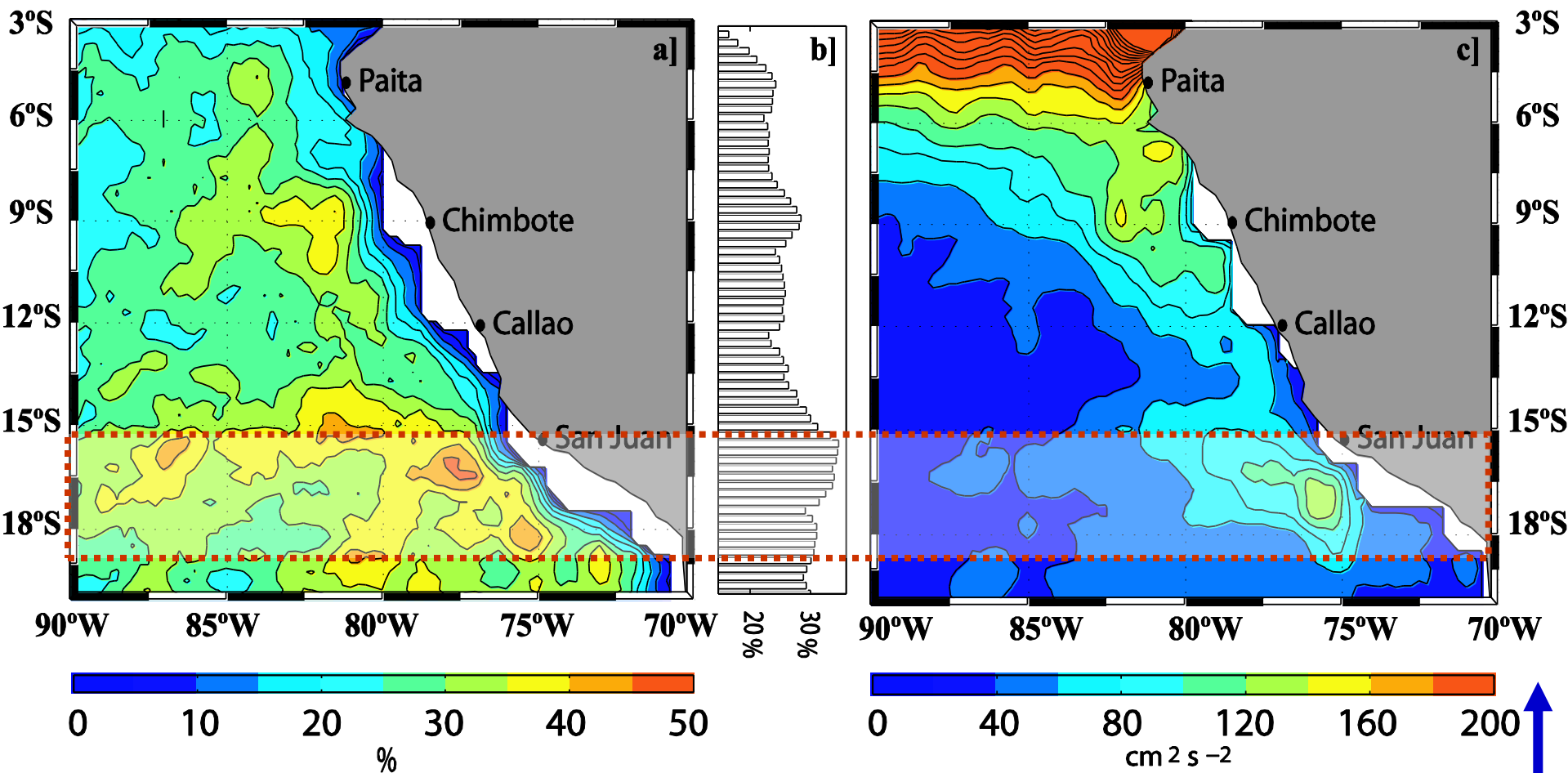
It provides information about the relative importance of strain and vorticity in the flow. This parameter (W) is defined as:

s_s - the shearing deformation rate,
 s_n - the straining deformation rate and
 ω - vorticity

$$W = s_s^2 + s_n^2 - \omega^2$$

a) Climatología regional de la frecuencia de remolinos (%), Octubre 1992–Agosto 2006.

b) Variación meridional de la frecuencia promedio de remolinos (en %).



(c) Distribución espacial de la Energía Cinética promedio de los remolinos (EKE) (en $\text{cm}^2 \text{s}^{-2}$) de mediciones altimétricas.